energies

MDPI

Article

Reproducibility of Small-Format Laboratory Cells

Paul-Martin Luc *, Fabio Buchwald and Julia Kowal

Electrical Energy Storage Technology, Department of Energy and Automation Technology, Faculty IV, Secr. EMH 2, Technische Universität Berlin, Einsteinufer 11, D-10587 Berlin, Germany
* Correspondence: paul-martin.luc@tu-berlin.de; Tel.: +49-30-314-73859

Abstract: For the research and development of new battery materials, achieving high reproducibility of the performance parameters in the laboratory test cells is of great importance. Therefore, in the present work, three typical small-format lithium-ion cells (coin cell, Swagelok cell and EL-CELL ECC-PAT-Core) were tested and compared with regard to the reproducibility of their performance parameters (discharge capacity, internal resistance and coulombic efficiency). A design of experiments (DOE) with the two factors separator type and anode–cathode ratio (N/P ratio) was carried out for all cells. For the quality features discharge capacity, internal resistance and coulombic efficiency, the coefficient of variation is used as a measure of reproducibility. The statistical evaluation shows that in 83% of all cases, higher reproducibility is achieved when the Freudenberg separator is used instead of the Celgard separator. In addition, higher reproducibility is achieved in 78% of all cases if the anode and cathode are the same size. A general statement about which test cell format has the highest reproducibility cannot be made. Rather, the format selection should be adapted to the requirements. The examined factors seem to have an influence on the reproducibility but are more insignificant than other still-unknown factors. Since the production of small-format test cells is a manual process, the competence of the assembler seems to prevail. In order to mitigate the influence of as many unknown variables as possible, assembly instructions are proposed for each cell type.

Keywords: coin cell; test cell; reproducibility; design of experiments; cell assembly

Citation: Luc, P.-M.; Buchwald, F.; Kowal, J. Reproducibility of Small-Format Laboratory Cells. *Energies* **2022**, *15*, 7333. https://doi.org/10.3390/en15197333

Academic Editors: Mozaffar Abdollahifar and Arno Kwade

Received: 16 September 2022
Accepted: 3 October 2022
Published: 6 October 2022

1. Introduction

Extensive research and development are required to meet the continuous demand for high-quality batteries with new requirements. For the investigation of individual materials or entire cells, it makes sense to work with test cells that can have special sensors/connections, e.g., for temperature monitoring. Furthermore, test cells can be assembled by hand and can be disassembled for analysis if required. Since test cell housings are often reusable, costs can also be kept low.

Coin cells [1–3], Swagelok [4–6] and EL-CELLs (type: ECC-Std and PAT-Cell) [7–11] are most commonly used in laboratory studies. A reason why a specific cell format was chosen for the investigations is usually not given, since all three formats have been used in research for years.

Studies have already been conducted to maximize the reproducibility of the performance of the cell formats mentioned. While [12] focuses on the reproducibility of the PAT-Cell from EL-CELL, most of the literature refers to coin cell type R2032, which has been in use for over 35 years [13–16]. These investigations build on each other only slightly or not at all and sometimes even come to different conclusions. This complicates the selection of a suitable test cell format as well as its construction and use for future investigations. Considering the individual findings from the literature presented, this paper intends to compare the cell formats coin cell, Swagelok cells of two different sizes (big and small) and EL-CELL ECC-PAT-Core in terms of their reproducibility of cell performance.

2. Experimental

In this section, the utilized tools and materials as well as the three test cell formats coin cell, Swagelok cell (big and small) and EL-CELL ECC-PAT-Core, with the respective special features of the structure, are presented in more detail.

2.1. Tools and Materials

The cell assemblies used in this study consist of purchased anodes and cathodes coated on one side. An anode consists of an 18 µm thick copper foil and a 110 µm thick graphite coating. The cathode consists of a 20 µm thick aluminum foil coated with 212 µm Li-NMC oxide (lithium (nickel manganese cobalt) oxide). Two separators were used. The first is the FS3002 from Freudenberg and the second is the H2013 from Celgard. A mixture of ethylene carbonate (EC) and dimethyl carbonate (DMC) (percent by volume: 50/50) with 1 M of the salt lithium hexafluorophosphate ($LiPF_6$) is used as the electrolyte.

The cell assembly takes place under a protective atmosphere in a glovebox (M. Braun Inertgas-Systeme GmbH—UNIlab Pro Glove Box, Malsch, Germany) filled with argon gas. Round hollow punches of various diameters are used to punch out the electrodes and the separator. In addition to the hollow punches, a polyoxymethylene (POM) impact pad and a hammer are used. To ensure that the cell components are not damaged or cross-contaminated during assembly, three different ceramic tweezers with blunt ends are used for the anode, cathode and separator. A plunger-operated pipette from Eppendorf is used to apply the electrolyte, which can be set to values between 10 µL and 100 µL. The coin cells are crimped in the HCCCM-100 crimping machine from Xiamen Tmax Battery Equipments (Xiamen, China) with the housing cover (+) facing downwards.

The Swagelok cells must be screwed tightly with the nuts in the last assembly step. To ensure that the pressure from the plungers inserted into the housing remains constant during this time, the Swagelok cells are mounted in a self-constructed bracket. Appropriate wrenches or multigrip pliers are required for the nuts.

The finished cells are connected to the battery tester BTS-4000 from the company Neware Technology Limited (Hongkong, China), and the formation and cyclization are carried out in an oven (universal oven UF55 from Memmert, Büchenbach, Germany) to ensure a constant temperature.

2.2. Coin Cells

Figure 1a shows the utilized coin cell structure. According to [17], the spacer (thickness: 1 mm) is placed with the burr facing away from the anode–separator–cathode compound (ASC) as shown in Figure 1c (green check mark) to avoid damaging the anode. If the burrs face the separator (red cross), it is more likely that the ASC gets damaged. A total electrolyte quantity of 100 µL is used per coin cell to ensure that both the electrodes and the separator are completely wetted. During assembly, 50 µL is applied to the anode and 50 µL to the separator. Consequently, the amount of electrolyte is approximately 10% of the housing volume. A Freudenberg FS3002 with a diameter of 16.5 mm was used as the separator. The cathode is pressed lightly with the tweezers after placement to ensure the cathode does not float on the electrolyte and remains concentric to the anode during crimping. Table 1 shows the assembly sequence used and suggested.

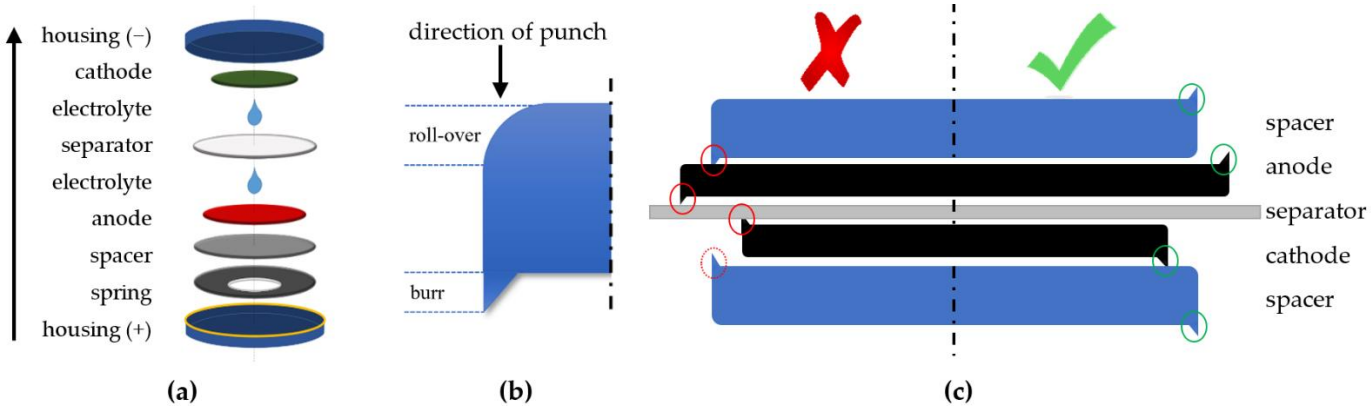

Figure 1. (**a**) Coin cell components and assembly order; (**b**) roll-over and burr of a punched disk; (**c**) assembly recommendations of punched cell components [17].

Table 1. Assembly instruction for coin cells.

Step	Instruction
1	Clean the work surface and set up all tools and cell components within easy reach. It is also advisable to place all passive cell components close to each other to keep the assembly time for all sub-steps as equal as possible.
2	The spring is inserted into the housing cover (−) with tweezers. If it is a disk spring, the larger radius of the spring points upwards. The spring should be placed as centrally as possible.
3	The spacer is placed on the spring. The same tweezers can be used for this. Care must be taken to position the spacer so that the burr of the spacer faces the spring. The spacer must be aligned concentrically with the spring.
4	The anode is placed on the spacer using tweezers or a vacuum pin. A single-side coated anode has the substrate facing the spacer and the active material facing up.
5	Half of the required amount of electrolyte is filled with a plunger-operated pipette (~50 µL) distributed on the anode. Complete wetting of the anode should be aimed for.
6	With the tweezers used for the spacer and spring, or with different tweezers, the separator or separators are now placed on the anode. This step can cause the anode to slip or the separator to float. If the anode and separator are non-concentric, the separator should be removed and repositioned.
7	The second half of the required amount of electrolyte (~50 µL) is distributed on the separator. Complete wetting of the separator should be aimed for. If two separators are used, a small amount of electrolyte can be applied between them.
8	The cathode has to be applied with a separate tweezer. For a single-sided cathode, the active material must point in the direction of the anode. To prevent the cathode from floating, the cathode can be gently pressed with the tweezers to suppress so much electrolyte that friction between the layers begins.
9	Now the housing (+) can be put on. This can be carried out with wide tweezers to ensure the case is placed parallel. The housing (+) should be pressed slightly to ensure friction between the cell components before rotating the cell for the crimping machine.
10	The coin cell is inserted into the crimping machine. A pressure of 950 psi is recommended. Small amounts of electrolyte may leak during crimping. The cell can be taken out and whipped clean. The crimping dye should also be wiped.

2.3. Swagelok Cell

The test cell comparison uses two different sizes of Swagelok cells as shown in Figure 2. With the smaller version, the diameter of the ASC can be as little as 10 mm in diameter. With the larger housing, it can be up to 12 mm. The middle parts of the housing (8) are made of metal and must be insulated against short circuits on the inside. A plastic film (7) made of biaxially oriented polyethylene terephthalate and a thickness of approx. 0.1 mm

is used, as the housing has an inside diameter of 10.3 mm or 12.2 mm. If possible, the insulating foil should cover the entire interior of the housing up to the clamping rings on each side. To insert the film into the housing, it must be brought into a cylindrical shape. In order to avoid a short circuit via the housing, the foil should be slightly larger than the inner circumference of the housing. The housings of both Swagelok cell sizes are identical in length. For the rectangular cut foils, the ideal dimensions of 25 mm (length) × 35 mm (circumference) for the small cell and 25 mm (length) × 41 mm (circumference) for the large cell have been found. Spacers (CuZn 37.6) with a diameter of 10 mm or 12 mm and a thickness of 1 mm are used to apply a homogenous pressure on the ASC. The spring (5) used for both Swagelok cell sizes is a helical compression spring (outer diameter: 9.9 mm; length: 20 mm; wire gauge: 0.9 mm; number of coils: 7). To exert pressure on the cell stack, an electrically conductive stamp (2) is inserted into the housing from both sides. The stamps have a diameter of 10 mm or 12 mm for the two case sizes. In order to be able to measure the Swagelok cells, the stamps have a thread on one side to enable contact via a screw connection. The stamps are connected to the housing with the aid of clamping rings (3 and 4) and hexagon nuts (1), and the inside of the housing is sealed off from the outside. The clamping rings come from Swagelok and are divided into front (4) and rear clamping rings (3). They are made of non-conductive nylon, polytetrafluoroethylene (PTFE) or perfluoroalkoxy alkane (PFA) to ensure insulation between the stamp and the housing and are designed for 10 mm and 12 mm tubing, respectively. The hexagon nuts are 19 mm or 22 mm (wrench size). Table 2 shows the assembly sequence used and suggested.

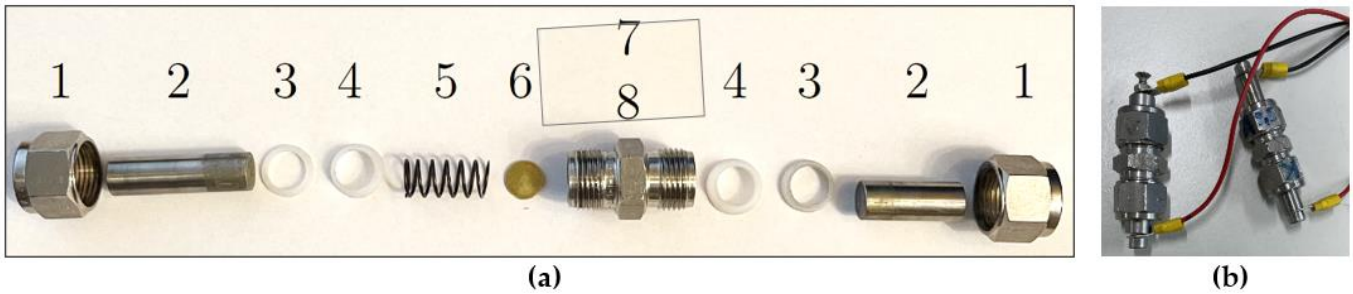

Figure 2. (**a**) Exploded view of a Swagelok cell; (**b**) Swagelok cell big (left) and small (right).

Table 2. Assembly instructions for Swagelok cells.

Step	Instruction
1	The insulating foil is shaped cylindrically by hand with the smooth side inwards and placed in the middle of the housing. The film can be carefully pressed onto the inside of the housing with one of the stamps so that there is no free space between the housing wall and the foil.
2	A front and a rear clamping ring are placed on the shorter stamp (cathode side), whereby the side with the smaller radius of the two clamping rings must point to the flat side of the stamp and not to the thread side. The front clamping ring is placed on the stamp so that the front part of the stamp is approximately 5 mm outside. The stamp is inserted into the housing and screwed tight with the nut.
3	The cathode is inserted with tweezers from the other side of the still-open case. In the case of single-sided electrodes, the active material faces upwards (towards the separator).
4	Half of the required amount of electrolyte (here: 50 µL) is evenly distributed on the cathode with a plunger-operated pipette.
5	The separator is placed on the electrolyte-covered cathode with a second pair of tweezers. The separator should be pressed lightly with the tweezers. The concentrically aligned separator can then be pressed lightly at the overlapping points of the separator on the housing wall.

Table 2. *Cont.*

Step	Instruction
6	The second half of the electrolyte (here: 50 µL) is applied evenly to the separator.
7	With a third pair of tweezers, the anode is placed on the separator with the active material facing down. During this step, extra care must be taken not to turn the anode the wrong way around when loosening it with the tweezers. A vacuum pin is recommended for this step.
8	The spacer is placed on the anode and lightly pressed.
9	The compression spring is placed on the spacer with the flat side down.
10	A front and rear clamping ring are placed on the longer stamp (anode side) with the same orientation as on the shorter stamp. This time, the front clamping ring is flush with the end of the stamp. The stamp is placed with the nut on the body and spring and the nut is tightened until the stamp can still be moved. After contact with the spring, the stamp is inserted 10 mm into the housing and the nut is tightened. To keep the compression of the compression spring the same, a torque wrench is recommended, with which the tightening torque can be adjusted. The tightening torque required should be determined in a preliminary test.

2.4. EL-CELL ECC-PAT-Core

In this study, the EL-CELL ECC-PAT-Core (EL-CELL) is used in the standard ECC-Std version, which allows testing of a two-electrode configuration without a reference electrode. The components of the cell are shown in Figure 3. The EL-CELL consists of a cell base (used as a positive pole, 3), a lid (used as a negative pole, 10), a non-conductive insulation sleeve consisting of two parts (5 and 7) into which the ASC is inserted, a lower (aluminum, 6) and an upper plunger (copper, 8), which act as spacers and transfer the compressive force evenly to the ASC, a polyethylene sealing ring (4) between the cell base and the lid, which also serves as insulation to prevent a short circuit, a stamp with a gold-plated compression spring (9), which is placed in the lid, and the bracket (1), which presses the cell base and lid together via a screw connection and at the same time exerts pressure on the ASC via the stamp on the spring.

Figure 3. EL-CELL ECC-PAT-Core components.

The contact for the reference electrode (2) is tightly screwed into the cell base but is not connected to any reference electrode. The separator is clamped between the two components of the insulation sleeve and is therefore significantly larger in diameter than the electrodes inserted into the assembled sleeve. Testing different separator sizes has shown that a diameter of 21 mm is ideal so that the separator is not too big, making it uneven and not too small, making it not appropriately clamped and slipping out easily. The optimal maximum diameter of the electrodes was found to be 17.5 mm and thus does not correspond to the manufacturer's specification of 18 mm. At 18 mm, the electrodes were a bit uneven. Table 3 shows the assembly sequence used and suggested.

Table 3. Assembly instructions for EL-CELL ECC-PAT-Core.

Step	Instruction
1	The insulation sleeve is disassembled into its two parts, the separator is inserted into the larger half with tweezers and clamped by placing the smaller half on top.
2	In total, 50% of the electrolyte (here: 100 µL) is applied to the separator from the side of the larger half of the insulation sleeve using a plunger-operated pipette.
3	With a second pair of tweezers, the cathode is inserted with its active material facing the separator.
4	The lower aluminum plunger is inserted into the sleeve on the cathode.
5	The sleeve is inserted into the cell base with the lower plunge down. It should be noted that the sleeve is keyed and there is only one way the sleeve will fit into the cell base. If the sleeve is only slightly twisted, it jams and cannot be pushed all the way into the cell base.
6	The second half of the electrolyte is applied to the other side of the separator.
7	With a third pair of tweezers, the anode is placed on the separator with the copper side up.
8	The upper plunger is inserted into the sleeve.
9	If not already carried out, the stamp is inserted into the compression spring, and then the stamp and the compression spring are placed on the upper plunger.
10	The sealing ring is placed on the cell base.
11	The lid is placed on the stamp with the spring and pressed down slightly, allowing the entire cell to be inserted into the bracket.
12	Finally, the housing is closed with the wing nut of the bracket. The screw is turned until a clear resistance can be felt, and the screw ends exactly in the middle turning position.

2.5. Wetting, Formation and Cyclic Aging

The assembled test cells were placed in a temperature chamber at 30 °C. Connected to the battery tester, each cell format started with a resting phase of 12 h to ensure the electrolyte reached all pores. Since this paper focuses on comparing reproducibility instead of achieving the best possible performance, the formation was performed with only one CCCV (CC: constant current; CV: constant voltage) charging cycle. For the CC phase, a current of C/10 to 4.2 V was chosen, and for the CV phase, a stop current of C/50 was chosen. After a 10 s resting phase, the cyclic aging began. With a current of C/2, the cells were charged and discharged for 30 cycles between 2.5 and 4.2 V, as shown in Figure 4.

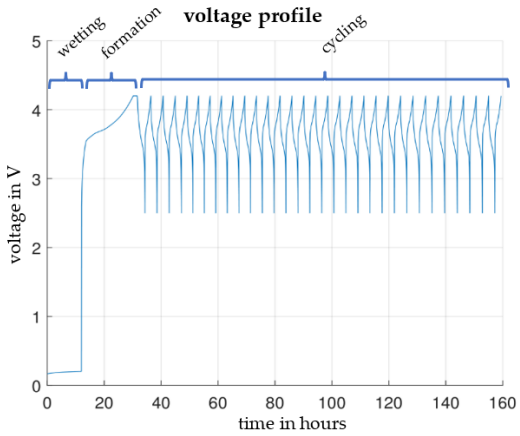

Figure 4. Voltage profile for wetting, formation and cyclic aging.

3. Results

For each cell format, a 2^2 full factorial experiment was performed. The factors separator type (Freudenberg FS3002 (+); Celgard H2013 (−)) and cathode–anode ratio (N/P ratio; N/P ratio = 1 (+); N/P ratio > 1 (−)) were examined.

Since hollow punch diameters are usually only available in 0.5 or 1 mm increments, it was impossible to achieve a fixed N/P ratio for all cell formats. According to [16], an N/P ratio of 1.15 is recommended. It was also stated that larger ratios lead to lithium losses over a large number of cycles. However, this can be neglected here since only the first five cycles were considered.

Because the production of all test cells is a manual process that requires fine motoric skills and an understanding of the processes, all tests were performed by one assembler who produced at least 50 cells in preliminary tests.

The quality features examined are the discharge capacity, the internal resistance and the coulombic efficiency (CE). Both the discharge capacity and the internal resistance were determined for the fifth cycle since the discharge capacities of all cells from the experiments only stabilized after the fifth cycle due to the chosen formation. The CE best illustrates reactions with water or other foreign particles from the production process in the first few cycles of a lithium-ion battery [18,19]. For this reason, the CE, the ratio of the amount of charge removed to the amount of charge introduced, is particularly suitable for assessing the quality of the electrode coating, cell structure and electrolyte filling and distribution. Since the charge loss is most pronounced in the first cycle of the experiment and then quickly approaches 100%, this performance parameter was only recorded in the first cycle.

The empirical coefficient of variation $VarK$ was used as a measure for evaluating the reproducibility. It is defined by the quotient of the empirical standard deviation (s) and the arithmetic mean of the measurements X ($\overline{X}$) according to Formula (1).

$$VarK(X) = \frac{s}{\overline{X}} \tag{1}$$

Table 4 shows an example of the 2^2-factor plan for the small Swagelok format with all three performance parameters.

Table 4. Measurement series for the small Swagelok cell.

Separator	N/P Ratio								
+Freudenberg −Celgard	+11.5 mm/11.5 mm (1) −11.5 mm/11 mm (>1)	Cell 1	Cell 2	Cell 3	Cell 4	Cell 5	$\overline{X}$	s	Var(X) in %
Discharge Capacity in mAh									
+	+	1.98	1.97	1.74	1.17	1.48	1.67	0.31	18.55
+	−	1.59	1.55	1.52	1.61	1.69	1.59	0.06	3.59
−	+	1.30	1.38	1.58	1.48	1.69	1.49	0.14	9.35
−	−	1.46	1.53	1.60	0.88	1.20	1.33	0.27	20.00
Internal Resistance in Ω									
+	+	32.29	34.51	39.49	36.85	18.78	32.38	7.21	22.28
+	−	41.71	50.73	57.27	50.83	44.74	49.06	5.41	11.02
−	+	45.96	92.52	65.11	51.10	42.63	59.46	18.22	30.65
−	−	31.22	44.83	28.07	59.09	67.96	46.23	15.46	33.43
Coulombic Efficiency in %									
+	+	67.07	63.96	62.49	51.14	55.73	60.08	5.81	9.66
+	−	61.10	60.62	58.85	59.86	63.51	60.79	1.56	2.57
−	+	57.44	50.25	59.52	53.90	61.79	56.58	4.10	7.24
−	−	57.70	62.92	61.79	14.73	28.15	45.06	19.82	43.99

Figure 5 shows the corresponding boxplots of all three performance parameters on the left (Figure 5a–c) and the coefficients of variation required for the comparison on the right (Figure 5d–f). In addition, only two instead of four boxplots are shown for the coin cell and the EL-CELL. Since the cathode and the anode in the EL-CELL fit perfectly and cannot slip, it was decided to change the separator as the only factor. Only one cell from

the coin cells made formation for each measurement series with the Celgard separator. For this reason, these two series of measurements are assessed as non-functional and are not taken into account in the further course of the evaluation.

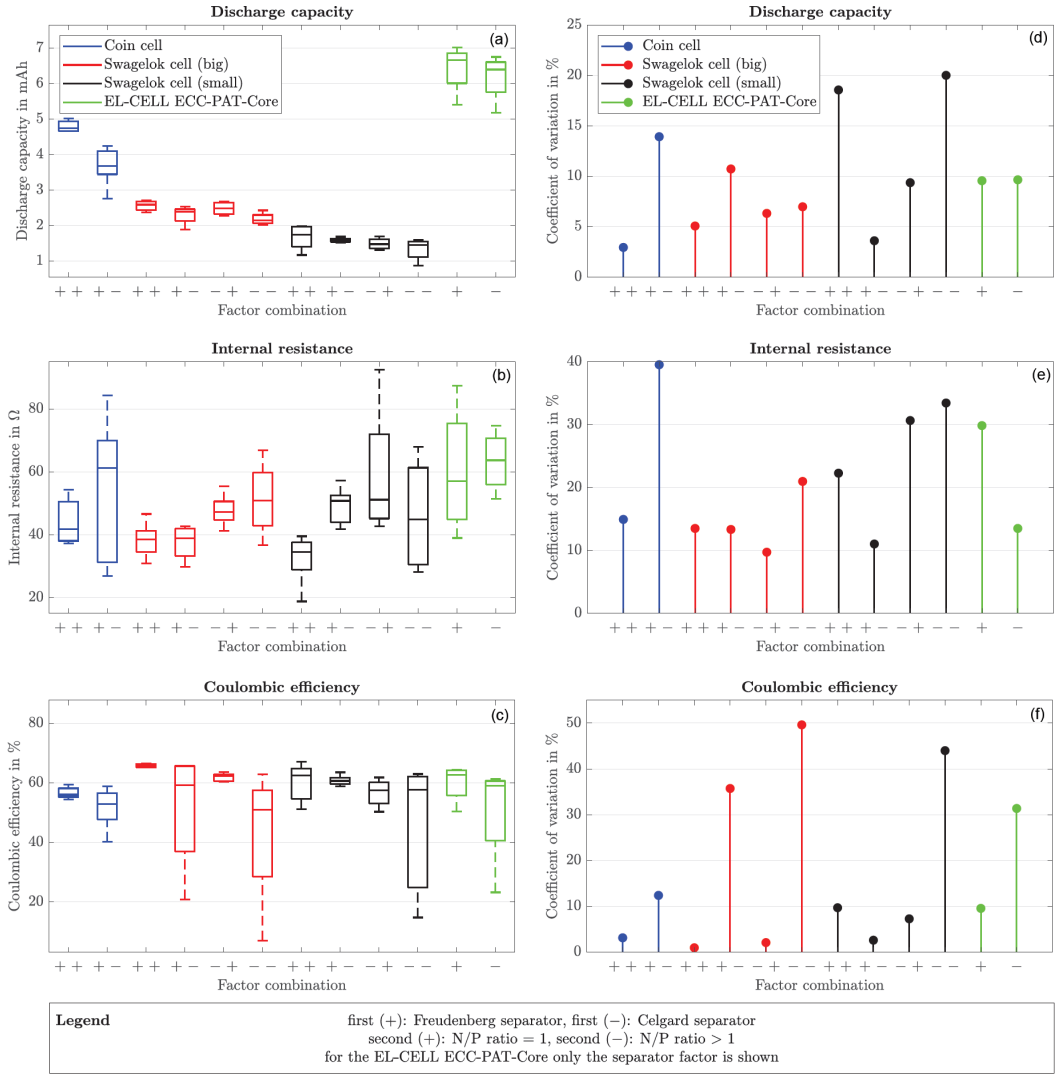

Figure 5. (**a**–**c**) Boxplots and (**d**–**f**) coefficient of variation for performance parameters of coin cell, Swagelok cell (big and small) and EL-CELL ECC-PAT-Core.

The apparent differences in the boxplot values are due to the different electrode sizes. However, when considering the coefficients of variation, it becomes clear that none of the cell formats considered has a low coefficient of variation for all three performance parameters. Instead, for each of the performance parameters considered, there is a cell format that performs better than the others.

3.1. Influence of Factor Combinations on the Discharge Capacity

Figure 5d shows that the coin cell with the Freudenberg separator and an N/P ratio of one has the highest reproducibility. The next best is the small Swagelok cell with the Celgard separator and an N/P ratio greater than one.

3.2. Influence of Factor Combinations on the Internal Resistance

Figure 5e shows that the large Swagelok cell with the Celgard separator and an N/P ratio of one has the highest reproducibility. The next best is the small Swagelok cell with a Freudenberg separator with an N/P ratio greater than one.

3.3. Influence of Factor Combinations on the Coulombic Efficiency

Figure 5f shows that the large Swagelok cell with the Freudenberg separator and an N/P ratio of one has the highest reproducibility. The next best is the large Swagelok cell with the Celgard separator with an N/P ratio of one.

The average of the coefficients of variation of all evaluable measurement series for the coin cell is 14.45%. The large Swagelok cell has an average coefficient of variation of 14.57%, while the small Swagelok cell has a value of 17.69%. The mean coefficient of variation for EL-CELL is 17.23%. The coin cell has the best average value. However, since the differences are not very large, the number of cells produced is small at five per factor combination and two measurement series of the coin cell were assessed as non-functional, it is not meaningful to claim which design generally has the greatest reproducibility.

A separate consideration of the factors in the form of main effect and interaction diagrams is more informative at this point.

To determine the effects of changing factor settings on systems, plots of the main effects, as shown in Figure 6a–c, can be derived from the corresponding coefficients of variation. When interpreting main effects plots, the steeper a line for a factor, the more influence that factor has on the system.

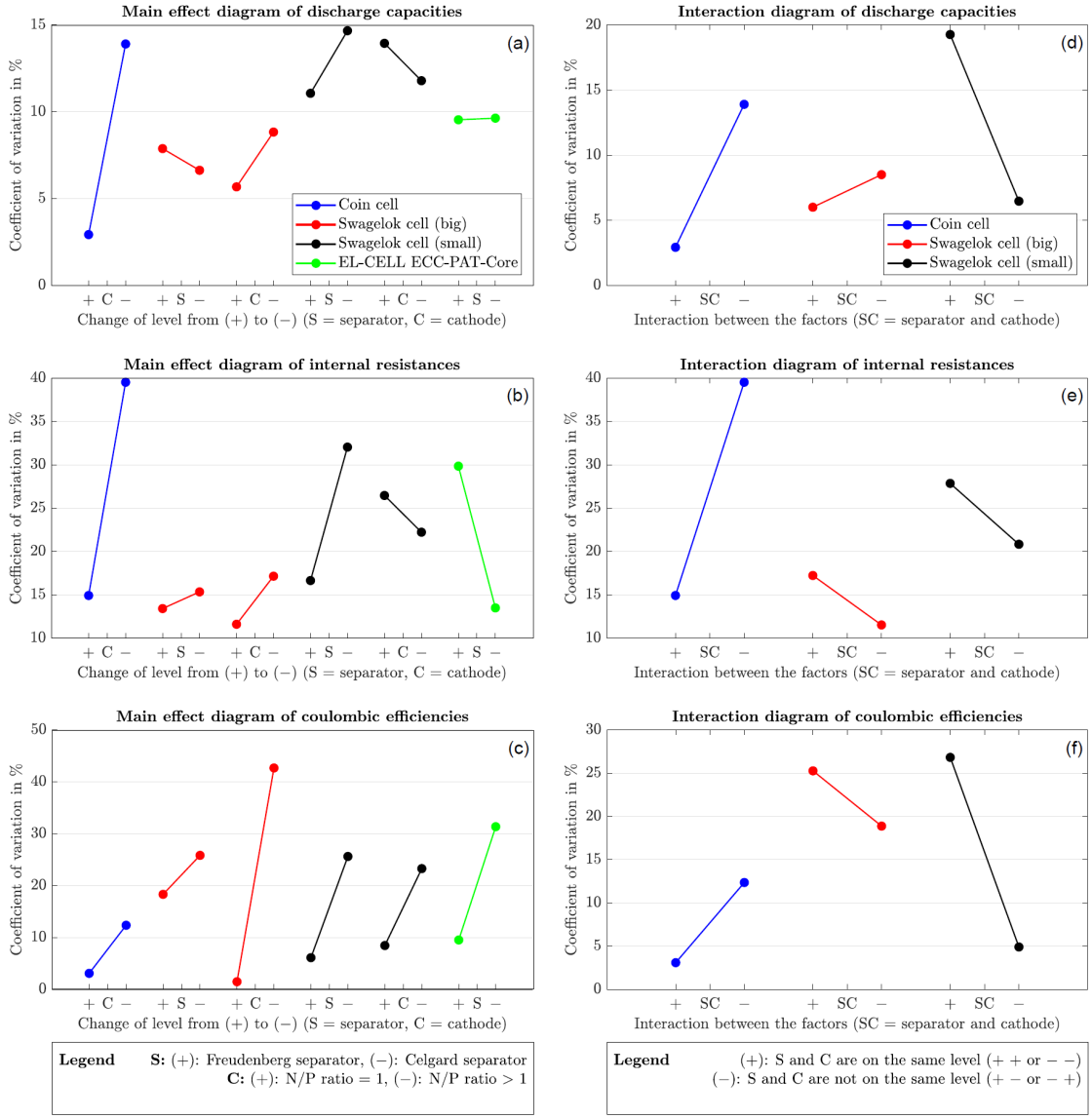

Figure 6. (**a**–**c**) Main effect diagrams for performance parameters; (**d**–**f**) interaction diagrams between the factor separator type and N/P ratio.

3.4. Influence of Individual Factors on the Internal Resistance

Figure 6b shows that the Freudenberg separator has higher internal resistance reproducibility in all cells except the EL-CELL. The separator type has the least impact on the large Swagelok cell. Looking at the N/P ratio, it turns out that the coin cell and the large Swagelok cell are more reproducible when the cathode diameter is equal to the anode diameter (N/P ratio = 1). In contrast, the small Swagelok cell gives better results with a smaller cathode diameter. The small Swagelok cell is also the least affected by the N/P ratio.

3.5. Influence of Individual Factors on the Discharge Capacity

The separator from Freudenberg has better values for the reproducibility of the discharge capacity (Figure 6a). The large Swagelok cell is the only test cell where the Celgard separator performs better. For the EL-CELL, the slope of the diagram is almost zero, which is why the choice of separator seems irrelevant here. If the N/P ratio of one is chosen, the reproducibility of the discharge capacity of the coin and large Swagelok cells is higher. The small Swagelok cell shows the least influence on the cathode size; here, an N/P ratio greater than one is advantageous.

3.6. Influence of Individual Factors on the Coulombic Efficiency

In all cases, the coulombic efficiency shows higher reproducibility when the Freudenberg separator is used (Figure 6c). Changing the separator when using the large Swagelok cell has the least influence on the reproducibility of the coulombic efficiency. Regarding the N/P ratio, all cases achieve better values with a cathode of the same size as the anode. Here, the coin cell is at least affected by the N/P ratio. However, it should be noted that all cells except the coin cell are cleaned and reused, while the coin cell housing, the spacer and the spring are always new. Since the degree of pollution is thus lower, the coin cell is favored when comparing the coulombic efficiency. It should also be noted that EL-CELL generally recommends changing the stamps for each cell structure.

Summarizing all the findings of the main effect diagrams, it is found that the separator from Freudenberg caused a higher reproducibility in 83% of the cases than the separator from Celgard. A similar picture emerges when choosing the cathode diameter. In 78% of the cases, an N/P ratio of one turns out to be beneficial.

3.7. Interaction between Factors

The selected experimental design also allows the interactions of the factors examined to be considered. They provide information about how much the reproducibility of the respective quality feature can change due to the factors' interaction and are presented in Figure 6d–f. The greater the slope of the diagrams, the more the interactions of the factors play a role in the reproducibility of the quality feature. The EL-CELL is not included in the graphs shown because it was only examined for one factor; thus, there is no interaction between the factors.

Figure 6d–f clearly shows that the interaction of the two factors examined has the least influence on the reproducibility of the three quality characteristics when using the large Swagelok cell.

4. Conclusions

This work dealt with the comparison of small-format lithium-ion batteries in terms of the reproducibility of their performance parameters. Since preliminary tests showed that both a tri-layer (PP/PE/PP; Celgard H2013) and a composite separator (PE/ceramic; Freudenberg FS3002) produced sufficiently functional cells in all designs, the separator type was chosen as a first factor in the presented main tests. In addition to the separator material, the anode–cathode ratio (1 and ~1.15–1.3) was given as a second factor. The quality characteristics that were examined for their reproducibility were the discharge capacity, the internal resistance and the coulombic efficiency. A total of four 2^2 full factor plans were performed with five cells per factor combination. The reproducibility was quantified by

the coefficient of variation. Due to the small differences, no general statement can be made as to which design has the highest reproducibility when considering the mean value of the coefficients of variation of all evaluable measurement series. Depending on the series of measurements, it turned out that the highest reproducibility of the internal resistance was achieved with the large Swagelok cell, the factor combination of the Celgard separator and the same size cathode as the anode. Regarding the discharge capacity, the coin cell with a Freudenberg separator and a cathode of the same size as the anode showed the best reproducibility. For the coulombic efficiency, the best result was the large Swagelok cell with the Freudenberg separator and using the same size for the cathode and anode. However, based on the main effect diagrams, it can be seen that in ten out of twelve cases (83%), the separator from Freudenberg showed better reproducibility values than the separator from Celgard. With regard to the cathode diameter, better results could be achieved in seven out of nine cases (78%) with the same diameter as the anode. It is noted that the factors considered are not critical to optimizing reproducibility. Instead, it could be shown that all three test cell formats considered are suitable for laboratory tests. It is assumed that parameters that have not yet been examined, such as the assembler's dexterity or fine motor skills, represent one of the greatest influencing factors on the reproducibility of test cells. For this reason, the assembler should not be changed in a series of measurements, or the assembly instructions should be as detailed as possible.

Author Contributions: Conceptualization, P.-M.L.; methodology, P.-M.L. and F.B.; software, P.-M.L. and F.B.; validation, F.B.; formal analysis, F.B. and P.-M.L.; investigation, F.B. and P.-M.L.; resources, P.-M.L. and F.B.; data curation, F.B.; writing—original draft preparation, P.-M.L. and F.B.; writing—review and editing, J.K.; visualization, P.-M.L. and F.B.; supervision, P.-M.L. and J.K.; project administration, J.K.; funding acquisition, P.-M.L. and J.K. All authors have read and agreed to the published version of the manuscript.

Funding: This research was funded by Deutsche Forschungsgemeinschaft (DFG), grant number KO4626/9-1. We acknowledge support by the German Research Foundation and the Open Access Publication Fund of TU Berlin.

Data Availability Statement: Not applicable.

Acknowledgments: The authors would like to thank Julian Long for incorporating all the measuring devices used here.

Conflicts of Interest: The authors declare no conflict of interest. The funders had no role in the design of the study; in the collection, analyses, or interpretation of data; in the writing of the manuscript; or in the decision to publish the results.

References

1. Radhika, M.G.; Byatarayappa, G.; Ingale, D.V.; Bhatta, L.K.G.; Venkatesh, K.; K, S.K.M.; Nagaraju, K. High performance of asymmetric coin cells designed using optimized weight percentage of multiwalled carbon nanotubes in Ni/Co-MOFs nanocomposites. *Mater. Res. Bull.* **2022**, *156*, 111996. [CrossRef]
2. Talaie, E.; Bonnick, P.; Sun, X.; Pang, Q.; Liang, X.; Nazar, L.F. Methods and Protocols for Electrochemical Energy Storage Materials Research. *Chem. Mater.* **2017**, *29*, 90–105. [CrossRef]
3. Wang, P.; Zhang, X.; Yang, L.; Zhang, X.; Yang, M.; Chen, H.; Fang, D. Real-time monitoring of internal temperature evolution of the lithium-ion coin cell battery during the charge and discharge process. *Extrem. Mech. Lett.* **2016**, *9*, 459–466. [CrossRef]
4. Muñoz-Rojas, D.; Leriche, J.-B.; Delacourt, C.; Poizot, P.; Palacín, M.R.; Tarascon, J.-M. Development and implementation of a high temperature electrochemical cell for lithium batteries. *Electrochem. Commun.* **2007**, *9*, 708–712. [CrossRef]
5. Rowden, B.; Garcia-Araez, N. Estimating lithium-ion battery behavior from half-cell data. *Energy Rep.* **2021**, *7*, 97–103. [CrossRef]
6. Vortmann-Westhoven, B.; Winter, M.; Nowak, S. Where is the lithium? Quantitative determination of the lithium distribution in lithium ion battery cells: Investigations on the influence of the temperature, the C-rate and the cell type. *J. Power Sources* **2017**, *346*, 63–70. [CrossRef]
7. Bach, T.C.; Schuster, S.F.; Fleder, E.; Müller, J.; Brand, M.J.; Lorrmann, H.; Jossen, A.; Sextl, G. Nonlinear aging of cylindrical lithium-ion cells linked to heterogeneous compression. *J. Energy Storage* **2016**, *5*, 212–223. [CrossRef]
8. Gabrielli, G.; Marinaro, M.; Mancini, M.; Axmann, P.; Wohlfahrt-Mehrens, M. A new approach for compensating the irreversible capacity loss of high-energy Si/C | $LiNi_{0.5}Mn_{1.5}O_4$ lithium-ion batteries. *J. Power Sources* **2017**, *351*, 35–44. [CrossRef]

9. Peng, C.; Lahtinen, K.; Medina, E.; Kauranen, P.; Karppinen, M.; Kallio, T.; Wilson, B.P.; Lundström, M. Role of impurity copper in Li-ion battery recycling to $LiCoO_2$ cathode materials. *J. Power Sources* **2020**, *450*, 227630. [CrossRef]
10. Sieg, J.; Schmid, A.U.; Rau, L.; Gesterkamp, A.; Storch, M.; Spier, B.; Birke, K.P.; Sauer, D.U. Fast-charging capability of lithium-ion cells: Influence of electrode aging and electrolyte consumption. *Appl. Energy* **2022**, *305*, 117747. [CrossRef]
11. Wagner, N.P.; Asheim, K.; Vullum-Bruer, F.; Svensson, A.M. Performance and failure analysis of full cell lithium ion battery with $LiNi_{0.8}Co_{0.15}Al_{0.05}O_2$ and silicon electrodes. *J. Power Sources* **2019**, *437*, 226884. [CrossRef]
12. Schmid, A.U.; Kurka, M.; Birke, K.P. Reproducibility of Li-ion cell reassembling processes and their influence on coin cell aging. *J. Energy Storage* **2019**, *24*, 100732. [CrossRef]
13. Murray, V.; Hall, D.S.; Dahn, J.R. A Guide to Full Coin Cell Making for Academic Researchers. *J. Electrochem. Soc.* **2019**, *166*, A329–A333. [CrossRef]
14. Long, B.R.; Rinaldo, S.G.; Gallagher, K.G.; Dees, D.W.; Trask, S.E.; Polzin, B.J.; Jansen, A.N.; Abraham, D.P.; Bloom, I.; Bareño, J.; et al. Enabling High-Energy, High-Voltage Lithium-Ion Cells: Standardization of Coin-Cell Assembly, Electrochemical Testing, and Evaluation of Full Cells. *J. Electrochem. Soc.* **2016**, *163*, A2999–A3009. [CrossRef]
15. Kayyar, A.; Huang, J.; Samiee, M.; Luo, J. Construction and testing of coin cells of lithium ion batteries. *J. Vis. Exp.* **2012**, e4104. [CrossRef] [PubMed]
16. Hu, J.; Wu, B.; Chae, S.; Lochala, J.; Bi, Y.; Xiao, J. Achieving highly reproducible results in graphite-based Li-ion full coin cells. *Joule* **2021**, *5*, 1011–1015. [CrossRef]
17. Luc, P.-M.; Bauer, S.; Kowal, J. Reproducible Production of Lithium-Ion Coin Cells. *Energies*, 2022; *in peer review*.
18. Korthauer, R. *Handbuch Lithium-Ionen-Batterien*; Springer: Berlin/Heidelberg, Germany, 2013; ISBN 978-3-642-30652-5.
19. Li, W.; Lucht, B.L. Inhibition of the Detrimental Effects of Water Impurities in Lithium-Ion Batteries. *Electrochem. Solid-State Lett.* **2007**, *10*, A115. [CrossRef]